Luminescence related to high density of Mg-induced stacking faults in homoepitaxially grown GaN

S. Khromov,[1,*] C. G. Hemmingsson,[1] H. Amano,[2] B. Monemar,[1] L. Hultman,[1] and G. Pozina[1]

[1]*Department of Physics, Chemistry and Biology (IFM), Linköping University, S-581 83 Linköping, Sweden*

[2]*Department of Electrical Engineering and Computer Science, Nagoya University, Chikusa-ku, Nagoya, 464-8603, Japan*

(Received 15 April 2011; revised manuscript received 30 May 2011; published 12 August 2011)

The effect of Mg doping on stacking fault (SF) formation in *c*-plane GaN grown by metal-organic chemical-vapor deposition has been studied for Mg concentration between 2×10^{18} cm^{-3} and 5×10^{19} cm^{-3}. Transmission electron microscopy studies demonstrate a direct correlation between the increasing Mg content and the number of small (3–10-nm long) SFs present. The energy dispersive x-ray analysis (EDX) line profile of a SF shows that the Mg-impurity atom resides at a distance approximately 5 nm from the SF. Cathodoluminescence (CL) mapping reveals that the Mg-doped regions radiate at energies corresponding to known SF emission peaks. SF-related peaks in CL spectra show metastability, which may be attributed to transfer processes involving Mg acceptors and nearby associated SFs.

DOI: 10.1103/PhysRevB.84.075324 PACS number(s): 61.72.Nn, 68.37.Og, 78.66.Fd, 78.60.Hk

I. INTRODUCTION

Mg is the most successfully and widely used element for *p*-type doping in GaN. Because of the high-activation energy, Mg concentrations exceeding $\sim 10^{19}$ cm^{-3} have to be incorporated in the material to obtain a reasonable hole conductivity at room temperature. Such high doping levels in *p*-type GaN, however, lead to the formation of structural defects, i.e., pyramidal inversion domains (PIDs), stacking mismatch boundaries, and spontaneous ordering,[1–3] which are detrimental to device performance and lifetime. Specifically, stacking faults (SFs) play the role of an additional potential for electronic confinement. In the vicinity of the dopant atom the charge carriers may be trapped at the SF, and impurity levels can be more localized in the band gap in the proximity of a SF.[4] Thus, Mg dopants can change their electronic properties in the presence of extended defects.[4,5] A high density of SFs is typical for undoped nonpolar GaN layers grown in the $\langle 11-20 \rangle$ direction (i.e., *a*-plane), where extended SFs of different geometry have been associated with cathodoluminescence (CL) peaks in the range of 3.29–3.41 eV. The emission at 3.41 eV has been commonly related to basal-plane SFs, luminescence attributable to prismatic SFs appears at $\sim$3.33 eV, while the 3.29-eV peak was associated with the partial dislocations-terminating basal-plane SFs (BSF).[6] CL spectra in the same spectral region, which could be correlated to structural defects as well as emissions related to acceptor-bound excitons, were surprisingly metastable, as previously reported for Mg-doped GaN layers with Mg concentrations in the range of 1×10^{19}–5×10^{19} cm^{-3}.[7–10] In this work we present results of structural and spectral analysis of homoepitaxially grown *c*-plane Mg-doped GaN layers with different Mg concentrations. It is demonstrated that metastable CL peaks can be related to nano-size SFs observed using transmission electron microscopy (TEM).

II. EXPERIMENTAL

Mg-doped GaN samples were grown by metal-organic chemical vapor deposition (MOCVD) homoepitaxially on *c*-axis GaN substrates. The freestanding substrates of 300-μm-thick GaN were fabricated by halide vapor phase epitaxy (HVPE) on (0 0 0 1) Al_2O_3 templates with subsequent removal of the sapphire. More detailed information about the HVPE substrates' growth process can be found in Refs. 11 and 12. The growth of each structure begins with a 0.5-μm-thick undoped GaN buffer layer followed by a Mg-doped GaN layer with the thickness of $\sim$1 μm. The growth temperature was 1050 °C and the growth pressure about 400 Torr. Ammonia, trimethylgallium and bis-cyclopentadienylmagnesium (Cp2Mg) were used as nitrogen, gallium, and magnesium precursors, respectively. Mg concentrations in the layers vary in the range 2×10^{18} cm^{-3} to 5×10^{19} cm^{-3}. Doping concentrations were estimated from growth conditions for which initial calibration was done using secondary ion mass spectroscopy (SIMS) analysis. Measurements were done on both as-grown samples and the same samples annealed at 800 °C for 10 minutes in nitrogen atmosphere. For comparison, an unintentionally doped *n*-type GaN layer grown homoepitaxially on a freestanding HVPE substrate at similar conditions was also studied. Cross-sectional TEM imaging, scanning transmission electron microscopy (STEM) imaging, and energy dispersive x-ray analysis (EDX) were performed with a high resolution FEI Tecnai G2 200 keV FEG instrument. TEM samples were thinned down to $\sim$10–50 nm to be electron transparent using mechanical polishing with subsequent ion milling in an Ar plasma. The spatial resolution of EDX scans in STEM measurements is $\sim$1 nm. CL measurements were done using a MonoCL2 system integrated with a FEG cathode LEO 1550 Gemini scanning electron microscope (SEM) and equipped with a cold-stage for temperature-dependent experiments in the range 5–300 K. The CL signal was dispersed using a 300-mm focal-length monochromator with an 1800 l/mm-diffraction grating and a spectral dispersion 2 nm/mm. The CL spectra were measured with an accelerating voltage of 15 kV, thus the penetration depth of electrons is $\sim$1 μm. A Peltier-cooled GaAs photomultiplier tube was used for data acquisition. The integration time was equal to 1 s per data point, and the detection time for one spectrum was approximately 3–4 min. The CL-peak intensities changed during the acquisition time; however, the metastability was rather slow, the

 ©2011 American Physical Society

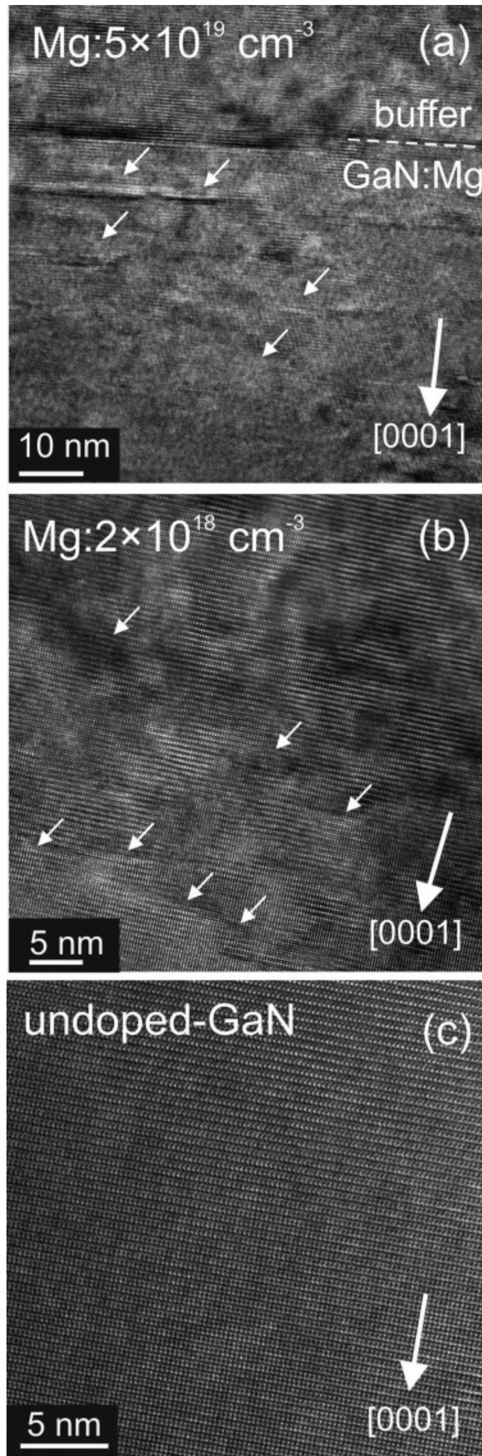

FIG. 1. Cross-sectional TEM images of GaN samples: (a) [Mg] = 5×10^{19} cm^{-3}, (b) [Mg] = 2×10^{18} cm^{-3}, and (c) undoped GaN. The white arrows indicate the position of SFs. The crystallographic direction [0001] is also indicated for each image.

main changes occurred within 30–60 minutes under electron irradiation.[8]

III. RESULTS AND DISCUSSION

TEM analysis was performed to clarify what kind of structural defects are present in the studied GaN:Mg samples. We find that incorporation of Mg in the GaN layers results in the formation of SFs with a very small typical length of 5–10 nm as it was revealed by TEM. Figure 1 shows cross-sectional TEM images of GaN layers with Mg concentration of (a) 5×10^{19} cm^{-3} and (b) 2×10^{18} cm^{-3}, while Fig. 1(c) demonstrates an undoped, i.e., unintentionally n-type doped, sample for comparison. White arrows indicate SFs. The crystallographic direction [0001] is also indicated on the images. While the SF density is slightly higher near the interface between the buffer and the layer, SFs were still observed within the whole Mg-doped film even close to the sample surface. To illustrate that, the interface region in the sample with a high Mg doping and the surface area in the layer with a low Mg concentration are shown in Figs. 1(a) and 1(b), respectively. The volume density of SFs is very high, comparable to the Mg concentrations, and it is enhanced with increasing doping. We have estimated the planar-SF density to $\sim 10^{11}$ and $\sim 10^{12}$ cm^{-2} in the samples with Mg-volume concentrations of 2×10^{18} and 5×10^{19} cm^{-3}, respectively. SFs were present in the samples with a rather low Mg concentration of 2×10^{18} cm^{-3} when GaN is still n-type. In contrast, unintentionally n-type-doped GaN layer grown without Mg at similar conditions exhibits no SF within the inspected area [Fig. 1(c)]. Thus, we conclude that incorporation of Mg atoms is correlated with formation of the small SFs (2–10 nm) with a high density.

Other structural defects identified as PIDs shown in Fig. 2 were observed only for GaN samples with Mg doping in the range of 2×10^{19} cm^{-3} or higher, which is consistent with observations of Vennegues *et al.*[1] The area density of PIDs was much less (at least two orders of magnitude) than that of SFs. Here, we will not discuss PIDs and their influence on optical properties of Mg-doped GaN.

To examine the type of SF a more detailed TEM image taken with higher resolution is presented in Fig. 3. The crystallographic directions were evaluated from the fast Fourier transform of the TEM image. We can establish that the observed BSF is of intrinsic type I_1, i.e., it corresponds to one interruption of the stacking sequence equivalent to change from ABAB stacking along [0001] into ABABCBC in the GaN epilayer with a total displacement vector $\frac{1}{6}\langle 20\bar{2}\bar{3}\rangle$. Here

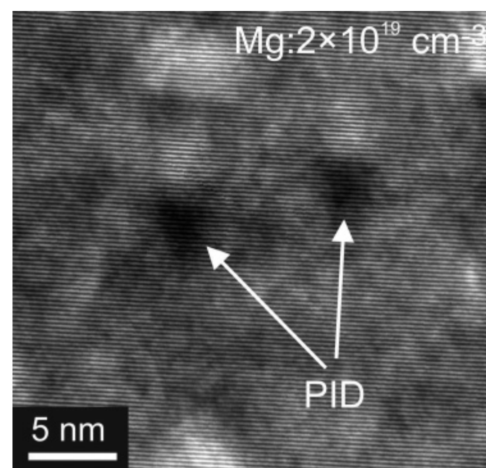

FIG. 2. TEM image of PID defects in p-type-doped GaN layer with Mg concentration 2×10^{19} cm^{-3}.

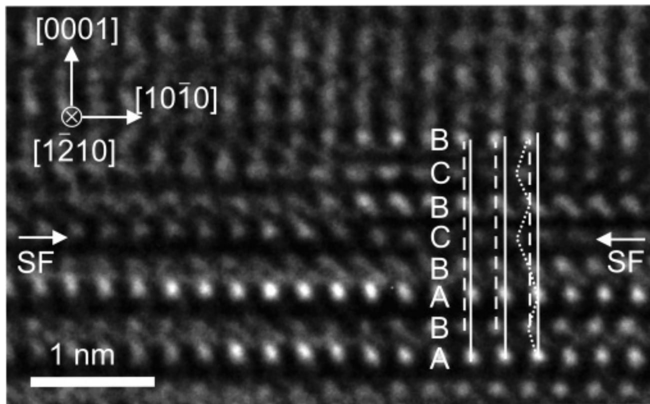

FIG. 3. TEM image of basal-plane SF in the as-grown sample with [Mg] = 5×10^{19} cm^{-3}.

the letters denote a double layer, and A, B, and C indicate the different atomic positions projected onto the (0001) plane. Despite the fact that the basal I_1-type of SF is the most common planar defect formed during the growth in GaN, we cannot exclude the presence of other types of defects, such as extrinsic basal-plane SFs, prismatic SFs, or dislocations of a different kind. For example, partial dislocations in wurtzite GaN delimit SFs of type I_1 as it was experimentally observed in Ref. 13. Prismatic SFs occur accordingly on prismatic $\{1\bar{2}10\}$ planes involving a lattice displacement of $\frac{1}{2}\langle 1\bar{1}01\rangle$ parallel to the fault plane.[14]

Since it is clear that Mg doping causes the SF formation in the GaN layer, it is interesting to know the relative position of the Mg atom with respect to a nearby SF. In order to study that, EDX-scan profiles and corresponding STEM images of basal-plane SFs were performed. The detection limit of the EDX detector was close to the Mg concentrations, thus, the signal/noise ratio was far from optimal. However, we could see a Mg-related peak in EDX profiles at the distance ~3–5 nm from the SF when the measurements were done across the basal-plane SF along the [0001] direction, as shown in Fig. 4(a). Figure 4(b) demonstrates EDX spectra taken at different distances relative to the SF, as indicated in Fig. 4(c), where the EDX scan trace is also shown by the white line. We could see the Mg-related peak in a rather localized space point close to the SF plane (~4 nm). Judging from the EDX signal strength we could not exclude possible clustering of magnesium atoms. This experimental result is in line with a theoretical work of Schmidt *et al.*[4] where calculations using density functional theory predicted that in wurtzite GaN it is more energetically favorable for a Mg atom to reside at some distance from the fault plane.

In order to activate the Mg-acceptors in GaN the samples were annealed (furnace annealing in N_2 at 800 °C for 10 min). We note here that from TEM analysis we have not observed any special difference regarding structural defects before and after the heat treatment. Thus, we assume that as-grown and annealed Mg-doped GaN samples possess a similar collection of SFs and other structural defects as formed during the growth.

The influence of structural defects on optical properties in Mg-doped GaN layers was studied by CL. Typical

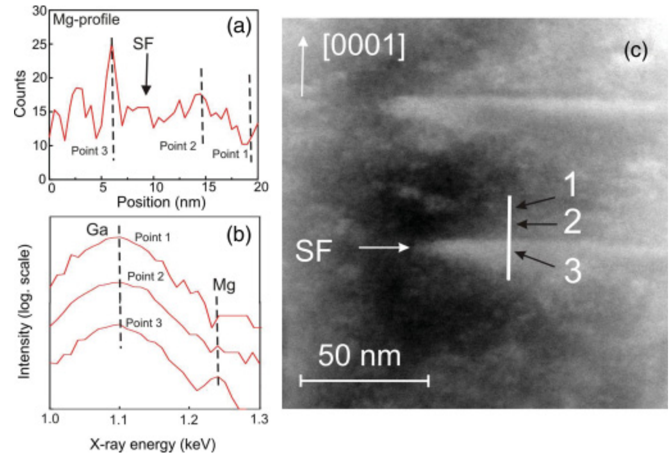

FIG. 4. (Color online) (a) EDX-line profile of Mg concentration in as-grown sample with [Mg] = 5×10^{19} cm^{-3}; (b) EDX spectra in the same sample from points 1, 2, and 3 as indicated in the STEM image in (c). The EDX scan was done over a SF as shown by the white line in (c). SF plane and the growth direction [0001] are indicated by arrows.

low-temperature CL spectra from GaN layers doped by Mg with different concentrations are shown in Fig. 5 for as-grown (solid lines) and annealed samples (dashed lines). Since the near-band gap luminescence is metastable, i.e., the spectral shape changes with time, the spectra were acquired right after the excitation, i.e., with delay time $\Delta t = 0$. The CL curves are normalized and shifted vertically for clarity. CL of a low-doped sample ([Mg] = 2×10^{18} cm^{-3}) is dominated by a strong emission at ~3.47 eV attributed to excitonic recombination. We cannot resolve all the lines, however, the main feature at ~3.476 eV is associated with excitons bound to residual Si and O donors, while acceptor-bound exciton (ABE) transitions occur at ~3.465 eV. According to previous results[10] this line, called ABE1, completely dominates the acceptor-related luminescence in low-doped GaN:Mg. The donor-bound exciton (DBE) intensity becomes negligible in the samples doped with higher Mg concentrations, while the emission related to the second acceptor-bound exciton

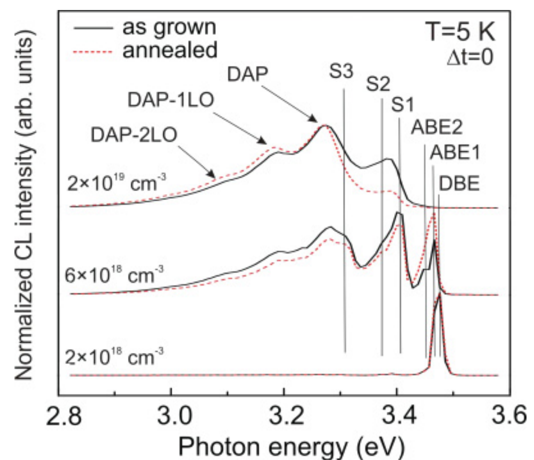

FIG. 5. (Color online) CL spectra taken at 5 K and $\Delta t = 0$ of Mg-doped GaN films before and after annealing with different Mg concentrations.

at ~3.454 eV (ABE2) appears. ABE1 and ABE2 lines are related to different Mg acceptors A1 and A2.[10] For higher Mg concentrations, a broad CL band from the donor-acceptor pair (DAP) recombination at ~3.27 eV increases together with its two longitudinal optical (LO) phonon replicas at ~3.18 and ~3.10 eV, respectively.

In CL we have detected several strong additional peaks between the bound-exciton transitions and DAP recombination, i.e., in the region 3.31–3.43 eV (Fig. 5). These features were not observed in photoluminescence (PL) spectra for *c*-plane GaN, even in the same Mg-doped layers. On the other hand similar lines related to structural defects were previously reported for *a*-plane GaN both in CL and PL spectra.[6,15,16] The difference between PL and CL spectra for *c*-plane Mg-doped samples may be explained by an increased probability of level activation in CL. A high-excitation density in CL may increase the electron's effective temperature at the bottom of conduction band, and consequently carriers can overcome a small potential barrier, which prevents electron occupation of the SF-related defect level in PL. In nonpolar *a*-plane GaN the following correlations were found: (i) between basal-plane SF and the emission at 3.41 eV (denoted as S1), (ii) between prismatic SF and the 3.33-eV luminescence, and finally, (iii) between the partial dislocations terminating basal-plane SF and the 3.29-eV peak.[6] Such a distinct assignment was possible because of a rather extended size of these defects (up to a few μm) in the *a*-plane samples.[6] In our Mg-doped *c*-plane GaN it is clear from TEM analysis that the length of most SFs is very small, not exceeding 10 nm. This excludes a direct comparison of the TEM images with the more poorly spatially resolved CL maps. The observed CL at 3.41 eV in the Mg-doped GaN layers can be assigned to the basal-plane SFs (denoted here S1), the peak at 3.37 may be associated with prismatic SFs (S2), and the 3.31-eV peak may be associated with partial dislocations (S3) by analogy with nonpolar GaN data.

It must be noted here, however, that while there is a consensus regarding the 3.41-eV line, there is still considerable debate going on about the origin of 3.29- and 3.32-eV peaks. Indeed, all authors in Refs. 6 and 17–19 assign 3.41-eV emission to BSF of type I_1. On the other hand Paskov *et al.* in Ref. 17 argue that the DAP-like behavior of 3.29-eV emission peak suggests that impurities incorporated in the partial dislocations rather than dislocations alone are responsible for this emission. The 3.35-eV emission was assigned by these authors to prismatic SF by analogy with Ref. 6. Gühne and coauthors in Ref. 18 state that 3.30- and 3.35-eV luminescence peaks come from areas with BSF, but prismatic SFs or partial dislocations were not visible there. Recently Tischer *et al.*[19] assigned the 3.32-eV line to I_2-type BSF by direct correlation of TEM and CL images. No prismatic SF or partial dislocations were found by these authors. Some discrepancy in the peak positions may be explained by different experimental conditions and the quality of the samples. From these references we can conclude that further research is needed to clarify the origin of 3.29–3.35-eV emission peaks.

ABE lines vanish very quickly under electron irradiation for as-grown samples with Mg concentrations above 2×10^{19} cm^{-3}, thus, only broadened spectral bands attributable to defects and DAP recombination are observed. Annealing in nitrogen activates the second acceptor in GaN, consequently the relative intensity of the ABE2 line increases in the annealed samples. Regarding the SF-related CL, no qualitative changes were detected in annealed samples, which is in line with the TEM characterization.

The metastability of near-band gap luminescence in the region 3.30–3.47 eV was previously studied in PL and CL for acceptor-bound excitons.[7–10] Relatively less attention, however, was paid to the CL peaks associated with structural defects. Figure 6 shows the temporal transformation of CL from samples doped with (a) moderate and (b) high Mg concentrations. CL spectra are taken directly after the excitation ($\Delta t = 0$) and at different times during continuous electron irradiation. The ABE1 line vanished with excitation time since the exciton is bound to the A1 acceptor, which is unstable under electron irradiation or ultraviolet excitation. In the annealed samples the ABE2 line is found to be more stable.[10] The observed metastability of the DAP recombination is also understandable since it is directly connected with metastable acceptors. However, unstable CL related to structural defects is more intriguing. Peaks assigned to SFs (S1–S3) are metastable, and the temporal evolution of their intensity depends on the Mg concentration. For moderately doped samples with [Mg] < 1×10^{19} cm^{-3}, we have observed, at first, a relative increase of the defect-related luminescence with corresponding reduction of the ABE intensity, and then a decrease of the S1–S3 lines relatively to the DAP signal. The S1–S3 peaks are getting

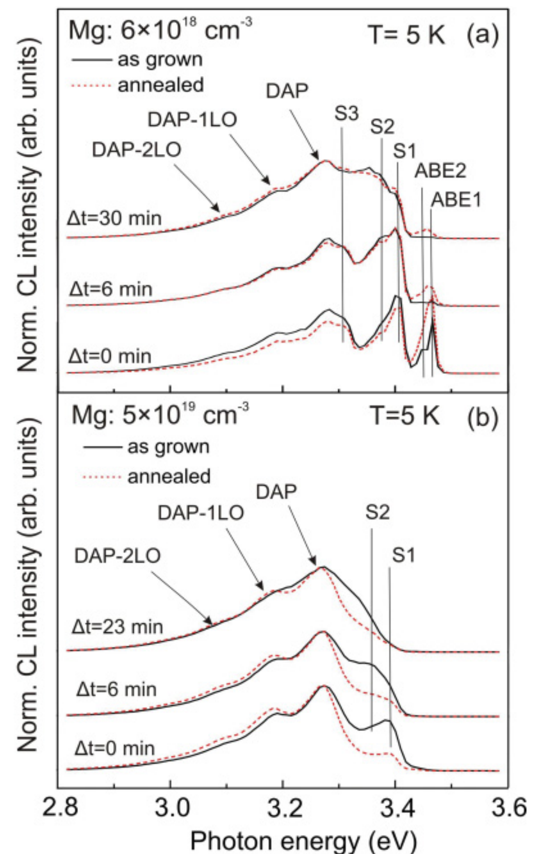

FIG. 6. (Color online) CL-spectra transformation during delay time $\Delta t = 0$–30 min at 5 K of Mg-doped GaN films with (a) [Mg] = 6×10^{18} cm^{-3} and (b) [Mg] = 5×10^{19} cm^{-3}. All spectra are normalized.

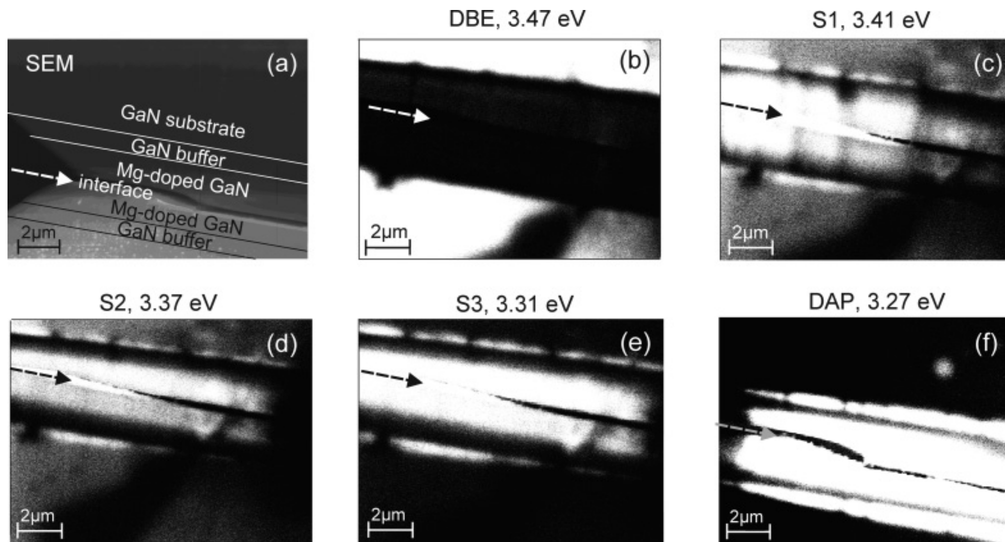

FIG. 7. (a) SEM and (b)–(f) CL mapping of a TEM sample for the as-grown Mg-doped GaN sample with [Mg] = 6×10^{18} cm^{-3}.

weaker for highly doped samples where no ABE lines are observed, and the DAP recombination dominates in CL spectra [see Fig. 6(b)].

To make sure that the S1–S3 peaks originate from the Mg-doped GaN layers, a spatially resolved CL mapping of the TEM samples was performed at selected photon energies. Figure 7(a) shows a SEM image together with a schematic drawing of the specimen for as-grown GaN layer doped with [Mg] = 2×10^{19} cm^{-3}, where the ABE line disappears within a few minutes after excitation while the intensity of the defect-related CL increases. Two pieces of the sample were put together surface-to-surface. The interface is indicated by an arrow in the SEM and all CL images in Fig. 7. At the energy position of 3.47 eV, which is associated with the DBE recombination, all luminescence comes from the GaN substrate having residual O and Si doping [Fig. 7(b)]. The brighter contrast in the maps correlates with the higher CL intensity. We can conclude from the difference in contrast in the maps taken at lower energies corresponding to the SF-related emissions [Figs. 7(c) and 7(d)] that the S1- and S2-related CL mainly comes from the Mg-doped layers, though a small part originates also from the GaN substrate. No defect-related CL comes from the undoped-GaN buffer. This fact can be understood in terms of the lower crystalline quality of the HVPE GaN substrates fabricated at a high growth rate (~200 μm/h) compared to the MOCVD GaN buffer grown with the rates of 0.5–1 μm/h. Thus, the GaN substrate has a higher SF density in comparison with the GaN buffer. The S3-related peak overlaps with the brighter Mg-related DAP recombination, and the CL-bright contrast corresponds to the Mg-doped GaN layers, as seen in Figs. 7(e) and 7(f), respectively. We note here, that because of the MOCVD growth routines, a small amount of Mg leaks into the reactor at the start of the buffer growth (confirmed by SIMS), which is manifested in the CL images by an additional bright line between the substrate and the buffer in Figs. 7(c)–7(f). Results shown in Fig. 7 justify the proposition that CL assigned to SFs can be correlated with defect formation in the epitaxial GaN attributable to Mg doping.

The question arises as to why the SF-related luminescence is metastable. As it follows from TEM analysis, the observed small SFs of high density in Mg-doped GaN are stable against the heat treatment at 800 °C, since we have not detected any difference between SFs in as-grown and annealed samples. We have not seen that the SF suffer changes because of accelerated electrons in TEM, thus, we can exclude that irradiation by electrons in CL can modify the SF structure. Then it is reasonable to assume that the energy of *e-h* pair recombination can not cause any mechanical transformation of SFs. However, CL data point out that the radiative recombination center related to the SF is sensitive to electron irradiation. We suggest the following recombination mechanism for excitons bound to SFs. The basal-plane SF can be considered as a ~3-monolayer-thin zinc-blende phase surrounded by wurtzite GaN.[5,20] The band potential is schematically shown in Fig. 8(a). Confinement for holes attributable to the small valence-band offset is only weak.[21,22] However, in the vicinity of the Mg acceptor, the SF potential can transform, as indicated in Fig. 8(b). In this case a hole is localized nearby in the wurtzite GaN and, thus, the SF can be considered as a radiative recombination center, provided it is occupied by an electron. Excitation of the SF may partly occur via exciton transfer from the nearby Mg acceptor, explaining the rapid initial quenching of the ABE1

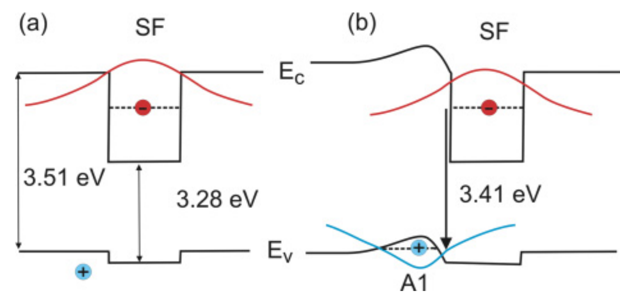

FIG. 8. (Color online) (a) Schematic drawing of the band alignment in the case of basal plane SF. (b) Band profile in the vicinity of the acceptor.

CL (Fig. 6). The decrease of the SF-related CL intensity at longer times (Fig. 6) may be explained as a slow-transfer effect of excitons and/or holes from the activated SF to more distant defects. The issue concerning the detailed interaction between a Mg acceptor and a SF just 3 nm away is interesting not only from a fundamental point of view but also from the point of view of device efficiency and lifetime.

IV. CONCLUSIONS

We have shown using TEM imaging that Mg incorporation in *c*-plane GaN results in SF formation. These defects were only observed in Mg-doped samples, their concentration being higher in samples with higher Mg content (up to the order 10^{12} cm^{-2}). At the same time even in low-doped GaN:Mg (about 10^{18} cm^{-3}), which is still *n*-type material, similar SFs with a considerable density have been found. The main structural defect was identified to be of I_1 basal-plane SF type. EDX analysis revealed that the impurity Mg atom is situated about 3–5 nm from the SF plane. CL spectra from moderate to high Mg-doped samples exhibit several SF-related peaks in the 3.3–3.41 eV range and show metastability. Spatially resolved CL mapping taken at energies corresponding to the transitions assigned to structural defects confirmed that the observed luminescence comes mostly from the Mg-doped regions of the samples. The optical data suggest that these structural defects interact with the nearby Mg acceptors, and this interaction is suggested to be responsible for the observed metastability effects.

ACKNOWLEDGMENTS

This work was supported by the Swedish Energy Agency, the Swedish Research Council (VR), and the Swedish Governmental Agency for Innovation Systems (VINNOVA). We acknowledge J. Palisaitis for assistance with EDX measurements and Dr. P. Persson for useful discussion.

*s.khromov@gmail.com

[1] P. Vennéguès, M. Benaissa, B. Beaumont, E. Feltin, P. de Mierry, S. Dalmasso, M. Leroux, and P. Gibart, Appl. Phys. Lett. **77**, 880 (2000).

[2] J. E. Northrup, J. Neugebauer, and L. T. Romano, Phys. Rev. Lett. **77**, 103 (1996).

[3] Z. Liliental-Weber, M. Benamara, J. Washburn, I. Grzegory, and S. Porowski, Phys. Rev. Lett. **83**, 2370 (1999).

[4] T. M. Schmidt, R. H. Miwa, W. Orellana, and H. Chacham, Phys. Rev. B **65**, 033205 (2002).

[5] P. Corfdir, P. Lefebvre, J. Ristić, J.-D. Ganière, and B. Deveaud-Plédran, Phys. Rev. B **80**, 153309 (2009).

[6] R. Liu, A. Bell, F. A. Ponce, C. Q. Chen, J. W. Yang, and M. A. Khan, Appl. Phys. Lett. **86**, 021908 (2005).

[7] G. Pozina, B. Monemar, P. P. Paskov, C. Hemmingsson, L. Hultman, H. Amano, I. Akasaki, T. Paskova, S. Figge, D. Hommel, and A. Usui, Physica B **401-402**, 302 (2007).

[8] G. Pozina, P. P. Paskov, J. P. Bergman, C. Hemmingsson, L. Hultman, B. Monemar, H. Amano, and A. Usui, Appl. Phys. Lett. **91**, 221901 (2007).

[9] G. Pozina, C. Hemmingsson, P. P. Paskov, J. P. Bergman, B. Monemar, T. Kawashima, H. Amano, I. Akasaki, and A. Usui, Appl. Phys. Lett. **92**, 151904 (2008).

[10] B. Monemar, P. P. Paskov, G. Pozina, C. Hemmingsson, J. P. Bergman, T. Kawashima, H. Amano, I. Akasaki, T. Paskova, S. Figge, D. Hommel, and A. Usui, Phys. Rev. Lett. **102**, 235501 (2009).

[11] G. Pozina, C. Hemmingsson, J. P. Bergman, D. Trinh, L. Hultman, and B. Monemar, Appl. Phys. Lett. **90**, 221904 (2007).

[12] C. Hemmingsson, P. P. Paskov, G. Pozina, M. Heuken, B. Schineller and B. Monemar, Superlatt. Microstruct. **40**, 205 (2006).

[13] Ph. Komninou, J. Kioseoglou, G. P. Dimitrakopulos, Th. Kehagias, and Th. Karakostas, Phys. Stat. Sol. (a) **202**, 2888 (2005).

[14] J. Mei, S. Srinivasan, R. Liu, F. A. Ponce, Y. Narukawa, and T. Mukai, Appl. Phys. Lett. **88**, 141912 (2006).

[15] P. Corfdir, P. Lefebvre, J. Levrat, A. Dussaigne, J.-D. Ganière, D. Martin, J. Ristić, T. Zhu, N. Grandjean, and B. Deveaud-Plédran, J. Appl. Phys. **105**, 043102 (2009).

[16] P. Corfdir, J. Ristić, P. Lefebvre, T. Zhu, D. Martin, A. Dussaigne, J. D. Ganière, N. Grandjean, and B. Deveaud-Plédran, Appl. Phys. Lett. **94**, 201115 (2009).

[17] P. P. Paskov, R. Schifano, B. Monemar, T. Paskova, S. Figge, and D. Hommel, J. Appl. Phys. **98**, 093519 (2005).

[18] T. Gühne, Z. Bougrioua, P. Vennéguès, M. Leroux, and M. Albrecht, J. Appl. Phys. **101**, 113101 (2007).

[19] I. Tischer, M. Feneberg, M. Schirra, H. Yacoub, R. Sauer, K. Thonke, T. Wunderer, F. Scholz, L. Dieterle, E. Müller, and D. Gerthsen, Phys. Rev. B **83**, 035314 (2011).

[20] Z. Z. Bandić, T. C. McGill, and Z. Ikonić, Phys. Rev. B **56**, 3564 (1997).

[21] C. Stampfl and C. G. Van de Walle, Phys. Rev. B **57**, R15052 (1998).

[22] B. J. Skromme, L. Chen, M. K. Mikhov, H. Yamane, M. Aoki, and F. J. DiSalvo, Mater. Sci. Forum **457–460**, 1613 (2004).